Synthesis and Properties of Poly(ethylene terephthalate)/ Clay Nanocomposites by *In Situ* Polymerization

Se Hoon Kim,[1] Sung Chul Kim[2]

[1]*Daeduk Research Institute, Honam Petrochemical Corporation, 24-1 Jang-dong, Yuseong-gu, Daejeon 305-726, South Korea*
[2]*Center for Advanced Functional Polymers, Department of Chemical and Biomolecular Engineering, Korea Advanced Institute of Science and Technology, 373-1 Guseong-dong, Yuseong-gu, Daejeon 305-701, South Korea*

Received 8 December 2004; accepted 21 June 2006
DOI 10.1002/app.25120
Published online in Wiley InterScience (www.interscience.wiley.com).

ABSTRACT: Poly(ethylene terephthalate) (PET)/clay nanocomposites (PCNs) with *N*-methyl diethanol amine (MDEA)-based organoclays are synthesized by using *in situ* polymerization. Four kinds of MDEA-based materials are prepared and used as organifiers of pristine montmorillonite. The clay treated with the organifiers has a d-spacing range that is about 14–21 Å. The PCNs with these organoclays are characterized by using wide-angle X-ray diffraction, scanning and transmission electron microscopy, atomic force microscopy, capillary rheometry, and tensile and barrier testing. The PCNs form an intercalated and delaminated structure. The well-stacked nanoclays are broken down into small pieces in the PET matrix and the thickness of the clay bundle decreases to 20 nm. The melt viscosity and tensile strength of these PCNs increases with only 0.5 wt % clay. In oxygen barrier testing, the PCN with 1 wt % well-dispersed organoclay shows a twofold higher barrier property than pure PET. © 2006 Wiley Periodicals, Inc. J Appl Polym Sci 103: 1262–1271, 2007

Key words: organifier; organoclay; poly(ethylene terephthalate); nanocomposite; barrier property

INTRODUCTION

There have recently been several research studies on improving the properties and clay dispersion in poly (ethylene terephthalate) (PET)/clay nanocomposites (PCNs).[1–7] PCNs are mostly prepared by two processes: *in situ* polymerization or melt intercalation. In either process the modification of the pristine clay to enhance the compatibility with PET is the key technology.[8–10]

Modification involves the synthesis of the organifier that binds onto the silicate surface and increases the d-spacing of the clay gallery. The organifier treated clay (organoclay) induces intercalation of PET during polymerization.[11–13] However, most of the commercial organoclays are not suitable for PET because the organoclays are easily degraded and can induce side reactions of PET when the temperature is elevated to 290°C. Therefore, it is important to maintain the thermal stability of the organoclay in order to maintain its interlayer distance and organifier structure during PET polymerization and processing.

In this study we synthesized organifiers to improve the dispersibility of organoclay on a PET matrix during polymerization and modified pristine montmorillonite (MMT) with the organifiers. In addition, PCNs were prepared with these organoclays by *in situ* polymerization and the morphology and properties were investigated.

EXPERIMENTAL

Synthesis of organifier

Organifiers were made based on *N*-methyl diethanol amine (MDEA, 99%, Aldrich Chemical Co.). We classified the organifiers into four groups: MDEAs I–IV. MDEA I was MDEA itself, and MDEA II was synthesized by a two-step method described in our previous article.[14] First, isocyanate-terminated MDEA was prepared by reacting 2 equiv hexamethylene diisocyanate with 1 equiv MDEA by dropping MDEA in hexamethylene diisocyanate. Second, MDEA II was synthesized by dropping isocyanate-terminated MDEA in poly(ethylene glycol) under nitrogen at 65°C.

MDEA III and MDEA IV were synthesized by esterification of MDEA with adipic acid (99%, Aldrich Chemical Co.) and citric acid (99%, Aldrich Chemical Co.), respectively. MDEA III was prepared by synthesizing 2 mol adipic acid with 1 mol MDEA. The reaction was carried out under a nitrogen atmosphere at 220°C until the condensed water from the esterification

Correspondence to: S. C. Kim (kimsc@kaist.ac.kr).
Contract grant sponsor: Industrial Technology Development Fund, Korea Institute of Industrial Technology Evaluation & Planning.

Journal of Applied Polymer Science, Vol. 103, 1262–1271 (2007)

was completely removed. MDEA IV was synthesized by a process similar to MDEA III, but citric acid was used in this reaction instead of adipic acid. The schemes of these reactions are shown in Figure 1.

Preparation of organoclay

Cloisite Na^+ (cation exchange capacity = 92.6 mequiv/100 g, Southern Clay Products, Inc.) was used as the pristine MMT in this study. The first step of organoclay modification was quarternization of organifier in deionized water. The organifier was dissolved in deionized water at 60°C and concentrated HCl was dropped into the organifier solution to quarternize the amine group. The second step was preparing organoclay with quarternized organifier. The pristine MMT was dispersed in deionized water (2000 mL) at 60°C by using a mechanical stirrer. The organifier solution from the first step was poured into the suspension of pristine MMT, and the mixture was vigorously stirred with a mechanical stirrer for 24 h at 60°C. After the cation exchange process was completed, the mixture was filtered with a Buchner funnel and then washed with deionized water. These filtering and washing processes were repeated until there was no further formation of AgCl according to an $AgNO_3$ test to confirm the absence of halide anions. The organoclay was vacuum dried at 80°C overnight. Dried organoclay was ground with an IKA microfine grinder.

Synthesis of PCNs

PCNs were prepared by two-step melt-phase polymerization (esterification and polycondensation) in a 5-L pilot reactor. The monomers were purified terephthalic acid (Samsung Petrochemical Co. Ltd.) and ethylene glycol (Honam Petrochemical Corporation). A slurry mixture of monomers, additives, catalyst, and organoclay was prepared in each polymerization. The mole ratio of ethylene glycol to purified terephthalic acid was 1.3, and 30-ppm triethyl phosphate and 40-ppm cobalt acetate were used as additives in this reaction. Antimony(III) acetate (250 ppm) was used as a polycondensation catalyst. Organoclays or pristine MMT were added to the slurry mix.

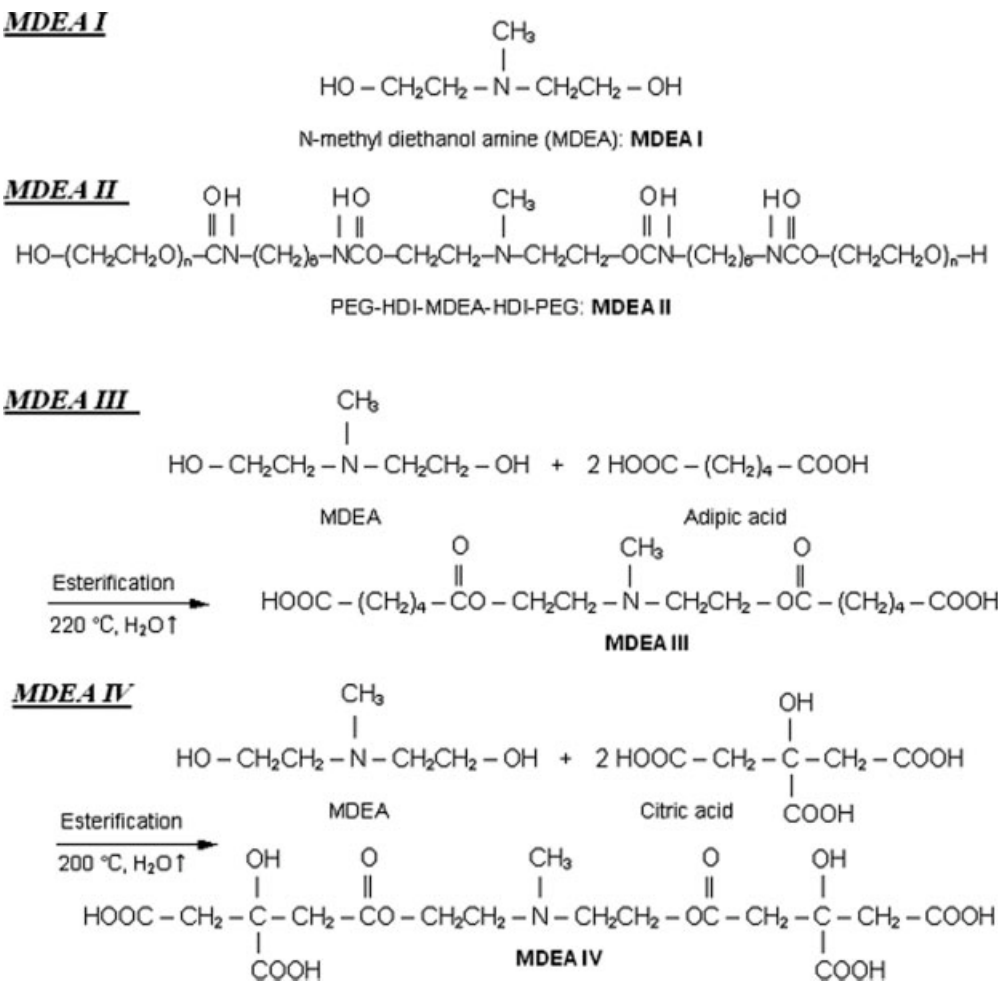

Figure 1 The reaction scheme for the synthesis of organifiers.

The slurry mixture was heated to 250°C under a nitrogen atmosphere for 5–6 h in the esterification step. It was transferred to a polycondensation reactor when the condensed water from esterification was completely removed. The temperature was raised to 285°C in the polycondensation reactor under vacuum conditions (0.5 Torr). The polycondensation step was continued for about 3 h until the intrinsic viscosity (IV) value of the PCNs reached 0.6 dL/g. The IV value was verified by the torque value of the agitator in our pilot reactor. After the polycondensation reaction was completed, the final product was extruded, quenched in a water bath, and then pelletized. According to the above method, four types of PCNs were finally prepared by *in situ* polymerization with four different organoclays: MDEA I, MDEA II, MDEA III, and MDEA IV.

Solid-state polymerization (SSP) and sheet processing of PCNs

Sheet samples were prepared by extrusion in order to measure the tensile properties, UV transmission rate, and gas barrier properties of PCNs. Generally, high molecular weight PET is needed (0.7–1.0 dL/g) for plastic containers or sheet products.[15] Therefore, the PCNs in this study were further polymerized by SSP before sheet processing.[16–18] The SSP process was composed of two steps: precrystallization and polymerization. The PCN pellets from the polycondensation reactor were placed in a 10-L tumbling reactor and the temperature of the reactor was elevated to 220°C through a precrystallization step at 145°C under 0.1 Torr for 3 h. The SSP was continued for about 8 h. The final IV value of the PCNs was increased to 0.8 dL/g after the SSP process. These products were processed with a multilayer sheet extruder (Create Plastic Co. Ltd.). The processing temperature was 270–285°C and the extruded sheet was quenched by several cooling rolls. The average size of a sheet was 120-mm width and 230-μm thickness.

Characterization

Thermogravimetric analysis (TGA) was performed under an air atmosphere using a TA Instruments Auto TGA 2950 to measure the thermal stability of the organoclays. The samples were heated to 900°C at a rate of 20°C/min. Wide-angle X-ray diffraction (WAXD) measurements were performed at ambient temperature on a Rigaku D/MAX-RC diffractometer with Cu Kα radiation to measure the d-spacing of the organoclays and PCNs. Each sample was scanned from 2θ 1.2–10° at a scan rate of 2°/min. The morphologies of the PCNs were investigated by scanning electron microscopy (SEM), atomic force microscopy (AFM), and transmission electron microscopy (TEM). SEM micrographs were obtained with a TOPCON SM-701. The vertical section of a PCN pellet was cut with a Leica microtome at room temperature, and then the specimen was prepared by two different methods. One was the general gold coating method, and the other was applied plasma etching on the vertical section of the specimen before gold coating. Plasma etching was conducted with a POLARON-PT7160 plasma reactor. The reflected power was 50 W and the specimen was treated within 7 min under 10^{-2} mbar. A POLARON SC7610 sputter coater was used to coat the microtomed and plasma etched surface of the pellet with gold. AFM is a convenient tool compared to SEM and TEM in the sense that sample preparation is simple and the phase information of the two-dimensional section area can be easily obtained.[19] AFM images were investigated with a Digital Instruments Nanoscope IIIa in tapping mode with standard etched silicon probe tips. The scanning frequency was 0.5 Hz and the scanner was type E. All the images shown here are phase images that were filtered through the Planefit procedure. SEM specimens were used as AFM specimens before a coating treatment with gold. TEM photographs were obtained with a Philips TECNAI F20 FEG using an acceleration voltage of 200 kV. TEM specimens were also created with a Leica microtome at room temperature. The apparent viscosity of the PCNs was measured at 280°C with an Instron UTM 4467/3210 RHEO. A capillary with a 0.7645-mm (0.0301 in.) diameter and 25.50-mm (1.0038 in.) length was employed. The extrudate velocity exiting the rheometer die was controlled by the crosshead speed, which ranged from 1.85 to 185 mm/min. The tensile properties for the PCN sheets were investigated with an Instron model 4466 machine according to ASTM D 638. Specimens conditioned at 50% relative humidity and 23°C were used for tensile testing. The crosshead speed was 300 mm/min. Barrier properties were investigated by UV and gas barrier. UV barrier property analysis was performed on a Lambda 40 UV/VIS spectrometer from PerkinElmer. The scan range was from 200 to 800 nm, and the scan speed was 240 nm/min. The gas barrier properties were represented by the oxygen transmission rate (OTR). The OTR was measured with a MOCON Oxtran 2/21 at 23°C and 0% relative humidity. The sample specification for OTR was a 120-mm^2 contact area and 230-μm thickness.

RESULTS AND DISCUSSION

Thermal behaviors

The thermal stability of an organoclay is dependent on an organifier because pristine MMT is generally degraded at about 600°C and the final loss of the pristine MMT at 900°C is less than 10%. The TGA results

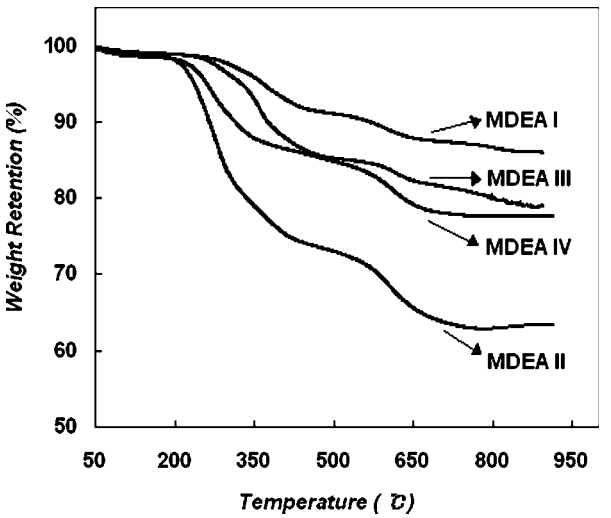

Figure 2 TGA thermograms of MDEA-based organoclays.

of the organoclays are shown in Figure 2 and summarized in Table I. The onset temperature of degradation and the temperatures of the maximum decomposition rate for the first stage and the second stage are represented as T_{OD}, $T_{max,1}$, and $T_{max,2}$, respectively. These results demonstrated that MDEA II organoclay was not suitable for preparing PCNs because its degradation temperature was lower than the temperature of PET polymerization (~290°C). The MDEA II organifier was unstable at that temperature, so the weight loss of MDEA II organoclay reached 15% at 290°C. The final residue of the MDEA II organoclay was only 63%. Especially when the PCN was polymerized with MDEA II organoclay, the final IV value did not reach the optimal value (0.6 dL/g) and discoloration of the PCN was observed. The MDEA IV organoclay had a relatively lower T_{OD} than the MDEA I and MDEA III organoclays, but the weight loss of MDEA IV was only 8% at 290°C and its degradation pattern was similar to that of MDEA III. The final residue of MDEA IV was around 78%, which was also similar to that of MDEA III (79%). In the case of using MDEA IV, PCN was successfully polymerized while maintaining transparency and reached normal IV values (~0.6 dL/g). The degradation temperatures of

TABLE I
TGA Results of Organoclays

Sample	T_{OD} (°C)	$T_{max,1}$ (°C)	$T_{max,2}$ (°C)	Residue (%)
MDEA I	303.1	368.6	595.8	85.94
MDEA II	224.7	275.2	375.5	63.28
MDEA III	308.7	360.1	620.0	79.04
MDEA IV	231.8	278.3	612.4	77.53

T_{OD}, onset degradation temperature; $T_{max,1}$, $T_{max,2}$, temperatures of the maximum decomposition rate for the first and second degradation stages, respectively.

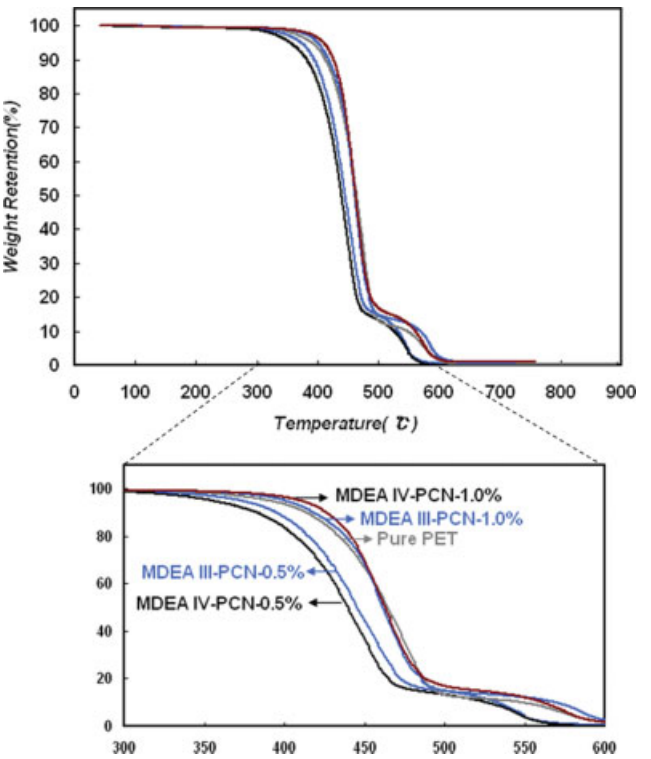

Figure 3 TGA thermograms of MDEA III–PCN, MDEA IV–PCN, and pure PET. [Color figure can be viewed in the online issue, which is available at www.interscience.wiley.com.]

MDEA I and MDEA III organoclays were higher than 290°C and the PCNs prepared with these organoclays also had normal IV values, but there was some discoloration on the MDEA I–PCN.

The thermal degradation patterns of MDEA III–PCN and MDEA IV–PCN display different behavior than a general nanocomposite, which retard the thermal degradation.[20,21] The degradation patterns of these PCNs are varied by changing the amount of clay loading. Both PCNs containing 0.5 wt % clay showed that the degradation patterns were moved to a lower temperature region compared to that of pure PET. In tzhe case of increasing amounts of clay, such as 1 wt % clay loaded PCNs, the thermal stability of the PCNs was increased and the degradation patterns were

TABLE II
TGA Results of MDEA III-PCN, MDEA IV-PCNs and Pure PET

Sample	Clay content (wt %)	T_{Di} (°C)	T_{D1} (°C)	Residue (%)
MDEA III-PCN	0.5	372.4	445.6	0.45
	1.0	400.3	461.7	0.83
MDEA IV-PCN	0.5	354.2	439.7	0.42
	1.0	409.9	462.8	0.85
Pure PET	0	390.4	464.6	0.21

T_{Di}, the initial degradation temperature at 5 wt % loss; T_{Dh}, the half-degradation temperature at 50 wt % loss.

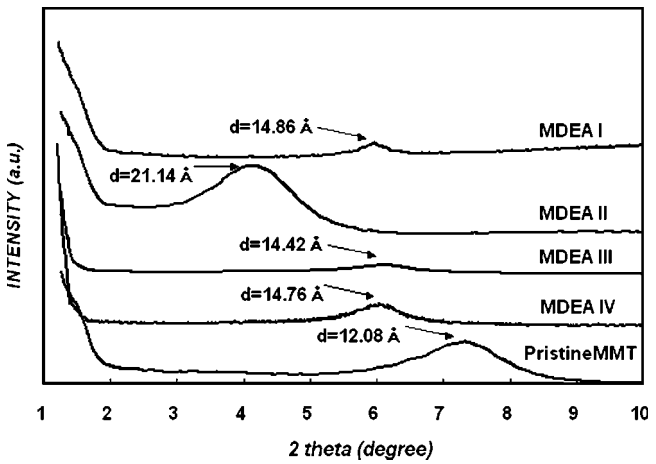

Figure 4 WAXD patterns for pristine MMT and MDEA-based organoclays.

shifted to a high temperature region. Figure 3 and Table II provide the TGA results of MDEA III–PCN, MDEA IV–PCN, and pure PET. The variation of the degradation pattern in the PCNs can be explained as an optimum amount of clay may exist to overcome thermal degradation that is due to low molecular weight materials in the organifiers.

WAXD

The d-spacing values of MDEA-based organoclays were checked by the WAXD patterns (see Fig. 4). The characteristic XRD peak of pristine MMT was found at 2θ 7.32°, which corresponds to an interlayer distance of 12.08 Å. The d-spacing value of the MDEA II organoclay was the largest at about 21.14 Å (2θ 4.18°). MDEA I, MDEA III, and MDEA IV organoclays had a similar d-spacing value of about 14 Å. MDEA I had a characteristic peak at 5.95° and d-spacing of 14.86 Å. MDEA III was 14.42 Å (2θ 6.13°), and MDEA IV was 14.76 Å (2θ 5.99°). These d-spacing values for MDEA I, MDEA III, and MDEA IV are smaller than other results for organoclays including long chains such as tallow[9,22,23] because MDEA organifiers (except MDEA II) have a relatively short chain length compared to general ammonium-based organifiers. However, the importance of the MDEA organifiers having hydroxyl and carboxyl end groups is the introduction of the reactive group that can react with monomers of PET, such as ethylene glycol and terephthalic acid, during *in situ* polymerization.

TABLE III
d-Spacing Values of Organoclays and PET/Clay Nanocomposites

Sample	2Θ	d Spacing (Å)	Clay content (wt %)
Organoclays			
MDEA I	5.95	14.86	—
MDEA II	4.18	21.14	—
MDEA III	6.13	14.42	—
MDEA IV	5.99	14.76	—
PET/clay nanocomposites			
MDEA I-PCN	5.92	14.93	0.5
MDEA II-PCN	6.11	14.47	0.5
MDEA III-PCN	6.01	14.71	0.5
MDEA III-PCN	5.89	15.01	1.0
MDEA IV-PCN	5.81	15.21	0.5
MDEA IV-PCN	6.02	14.68	1.0

Figure 5 shows the WAXD patterns of the MDEA II organoclay and MDEA II–PCN containing 0.5 wt % MDEA II organoclay. The d-spacing values of organoclays and PCNs are summarized in Table III. Despite the largest interlayer distance for MDEA II organoclay, the d-spacing value of MDEA II–PCN decreased to 14.47 Å (2θ 6.11°) after the polymerization process. This may have been caused by the degradation of the MDEA II organifier at the PET polymerization temperature. However, other PCNs (MDEA I–PCN,

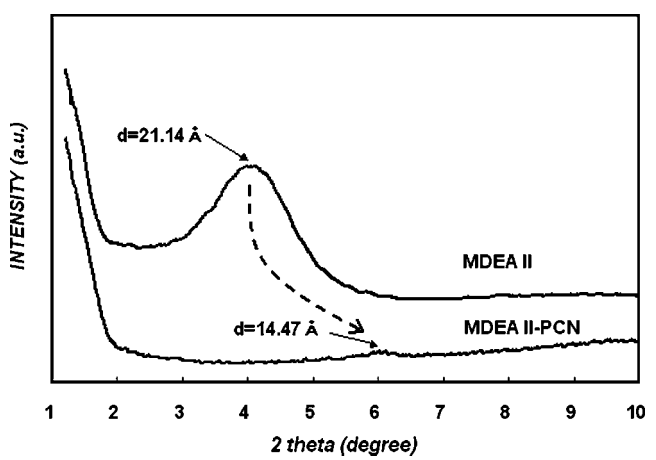

Figure 5 WAXD patterns of MDEA II organoclay and MDEA II–PCN.

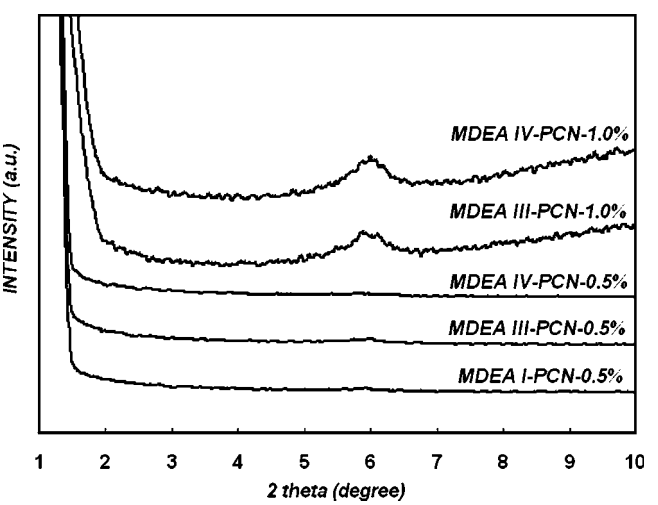

Figure 6 WAXD patterns of PCNs.

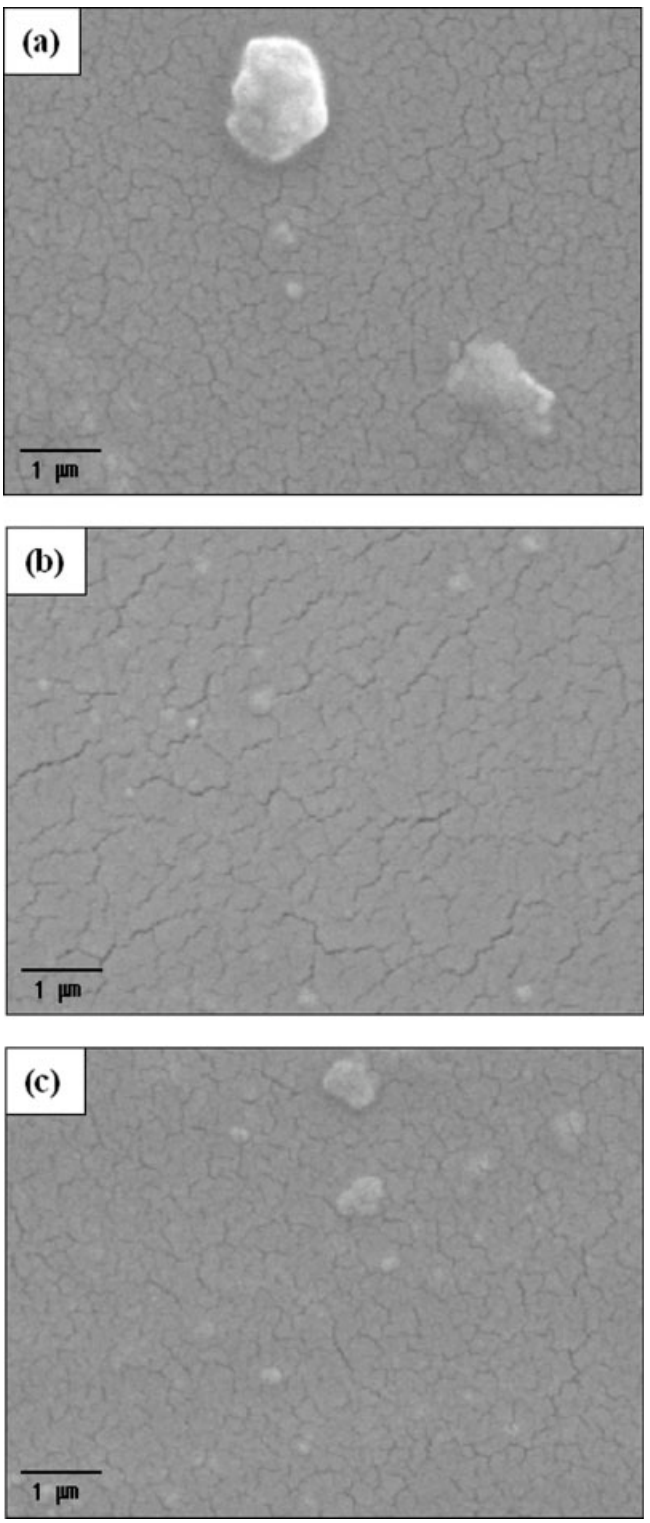

Figure 7 SEM micrographs of the PCNs with 0.5 wt % clay loading: (a) MMT–PCN, (b) MDEA III–PCN, and (c) MDEA IV–PCN.

MDEA III–PCN, and MDEA IV–PCN) had very weak diffraction peaks at around their organoclay's d-spacing value after polymerization, as shown in Figure 6. When increasing the clay contents to 1 wt %, the intensity of the peaks was slightly increased compared to the 0.5 wt % clay loaded PCNs, although the peaks were at nearly the same position as 0.5 wt % PCNs. These results demonstrate that there was no more collapse of the clay gallery from degradation of these

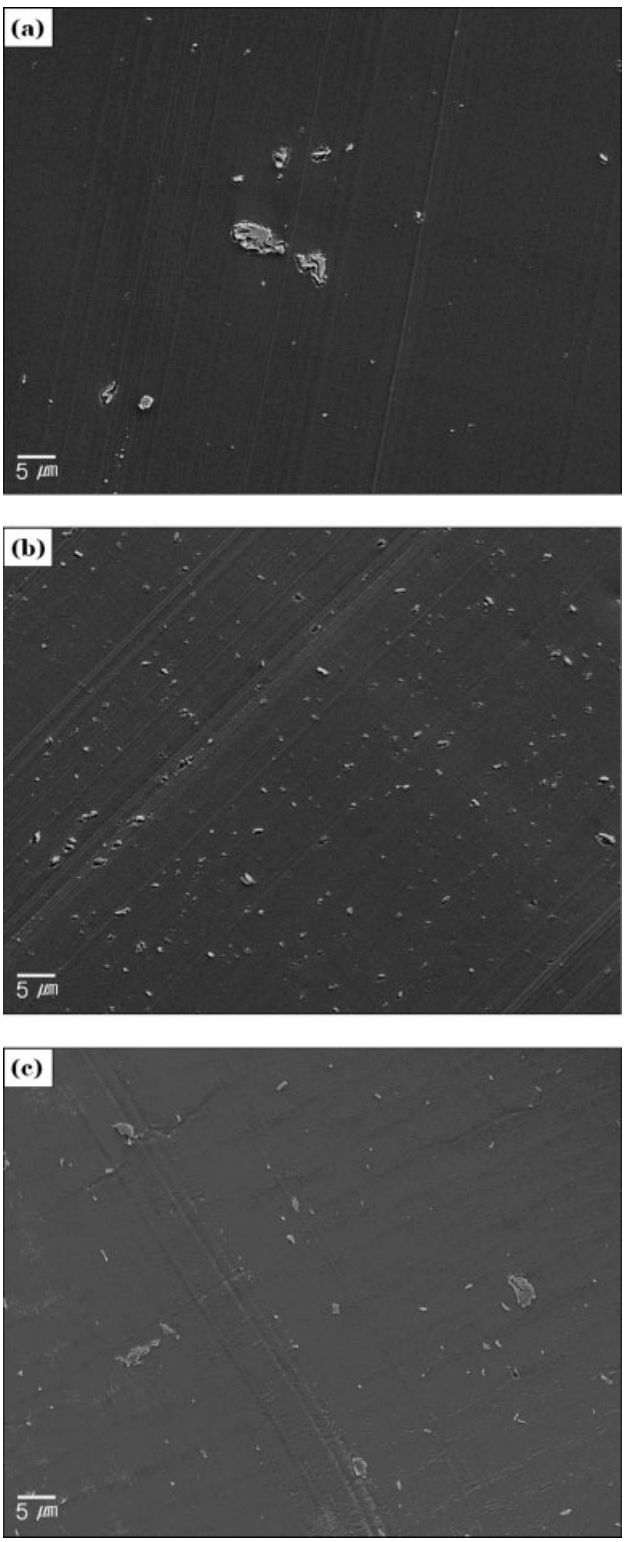

Figure 8 SEM micrographs of the plasma etched specimens of the PCNs having 0.5 wt % clay loading: (a) MMT–PCN, (b) MDEA III–PCN, and (c) MDEA IV–PCN.

organifiers during polymerization. However, the degree of intercalation and exfoliation in the PCNs could not be confirmed by these weak diffraction peaks because it is possible they originated from only a small amount of the aggregated clay in the PCN matrix. For this reason, it was necessary to check the morphology of the PCN because of the uncertainty of the WAXD data.

Morphology

The morphological investigation of this study was investigated with several microscopic methods. Samples were taken from MDEA III–PCN, MDEA IV–PCN, and MMT–PCN. The characterization of clay dispersion in the PCN can be divided into two categories, based on micron and submicron scales. From the viewpoint of a micron scale, SEM micrographs are generally used to study the overall dispersion state of the clay in the polymer matrix. The state of clay agglomeration can be classified by this micron-scale analysis. However, the intercalation and exfoliation structure of the clay are investigated by submicron-scale techniques, such as TEM.

Figure 7 presents SEM micrographs of MMT–PCN, MDEA III–PCN, and MDEA IV–PCN with 0.5 wt % clay loading. MMT–PCN is shown in Figure 7(a) and the MMT is shown as clay agglomerates with sizes of around 1 μm. The view of the dispersion of MMT in the PET matrix is not good. MDEA III–PCN shows a better dispersion state. The dispersed MDEA III organoclay is around 0.2 μm [Fig. 7 (b)]. MDEA IV–PCN shows intermediate clay dispersion between MMT–PCN and MDEA III–PCN; the agglomerated clay of the MDEA IV–PCN is around 0.5 μm [Fig. 7(c)]. These 1-μm scale images are not clear because the general gold coating in the preparation of the SEM specimen can cover the clay on the polymer surface. For that reason, the plasma etching method was also applied before gold coating in the specimen preparation. Figure 8 shows SEM micrographs of plasma etched samples of MMT–PCN, MDEA III–PCN, and MDEA IV–PCN with 0.5 wt % clay loading. These micrographs of plasma etched specimens can be more useful for studying clay dispersion than those of gold-coated only samples. The MMT–PCN shows large aggregated clay particles of about 5 μm, and there are very few small clay particles in the submicron region on the MMT–PCN in Figure 8(a). The micrograph of MDEA III–PCN [Fig. 8(b)] is quite different from that of MMT–PCN. Many clay particles existed at the submicron level and were well dispersed in MDEA III–PCN. Figure 8(c) provides a micrograph of the MDEA IV–PCN and the morphology indicates an intermediate state for clay dispersion between Figure 8(a) and Figure 8(b).

AFM measurements were conducted to attain additional information to the SEM results. The AFM images are presented in Figure 9. The AFM results are

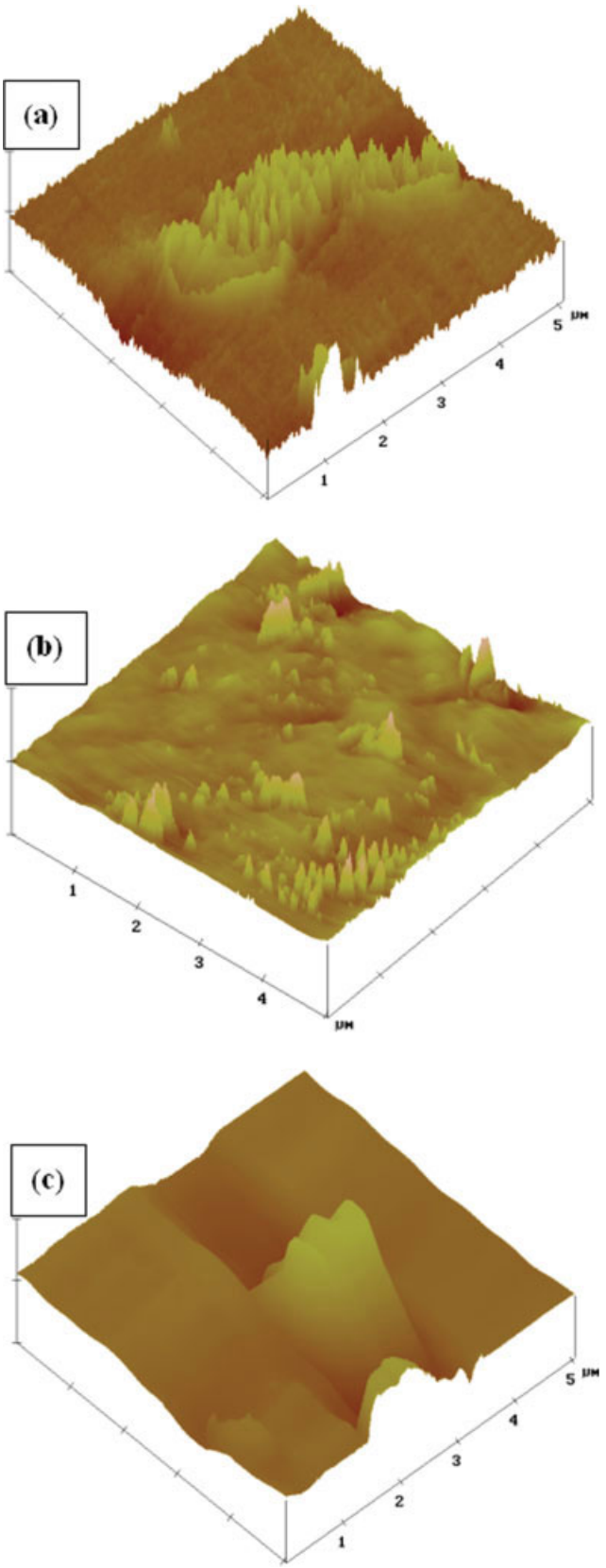

Figure 9 AFM images of PCNs: (a) MMT–PCN, (b) MDEA III–PCN, and (c) MDEA IV–PCN. [Color figure can be viewed in the online issue, which is available at www.interscience.wiley.com.]

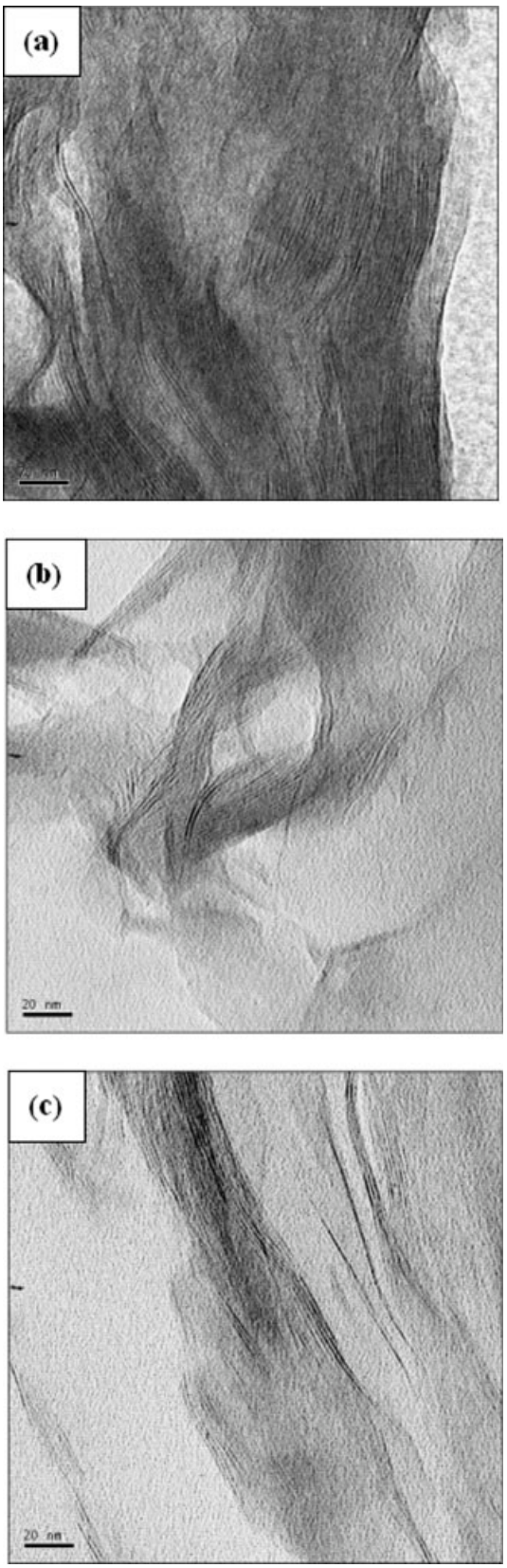

Figure 10 TEM micrographs of (a) MMT–PCN, (b) MDEA III–PCN, and (c) MDEA IV–PCN.

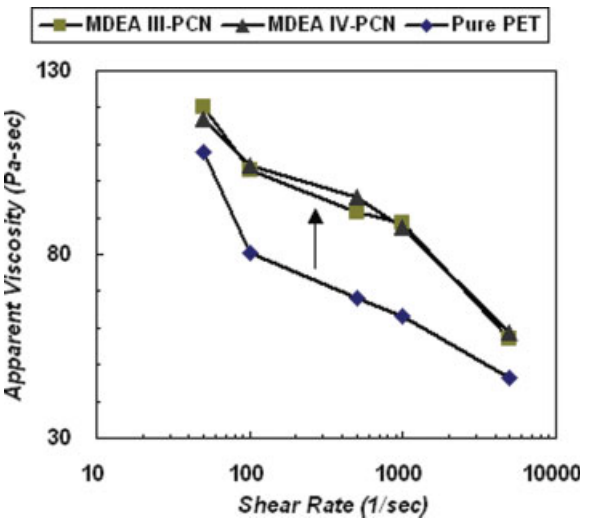

Figure 11 The apparent viscosity versus the shear rate of MDEA III–PCN, MDEA IV–PCN, and pure PET at 280°C. [Color figure can be viewed in the online issue, which is available at www.interscience.wiley.com.]

very similar to the patterns of clay dispersion in SEM. Figure 9(a) shows MMT agglomeration in the MMT–PCN. The size of agglomerated MMT was about 5 μm, which was larger than that of the SEM result in Figure 7(a). The MDEA III–PCN shows a big improvement in clay dispersion. We found that MDEA III organoclay was dispersed very well on a submicron scale in the PET matrix [Fig. 9(b)]. MDEA IV–PCN showed an intermediate dispersion state [Fig. 9(c)].

TEM micrographs are provided in Figure 10 to supplement the qualitative information of the nanoclay layers in the PCN. Figure 10(a) shows large nanoclay bundles in the MMT–PCN with a thickness of over 100 nm; there are well-stacked nanoclays without much delamination. In the case of MDEA III–PCN [Fig. 10(b)], we observed delaminated clay sheets in the matrix. The thickness of the nanoclay bundle

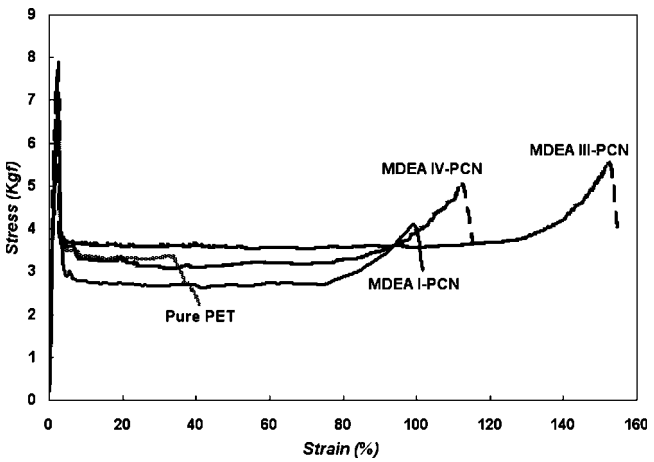

Figure 12 Stress–strain curves of pure PET, MDEA I–PCN, MDEA III–PCN, and MDEA IV–PCN.

TABLE IV
Tensile Properties of Pure PET and 0.5 wt % Clay Loading PCNs

Sample	Yield stress (kgf)	Yield strain (%)	Tensile strength (MPa)	Fracture stress (kgf)	Fracture strain (%)
Pure PET	6.77 ± 0.64	2.17 ± 0.27	27.50 ± 5.96	2.23 ± 0.75	40.67 ± 14.87
MDEA I-PCN	6.12 ± 0.44	2.69 ± 0.31	49.36 ± 3.31	4.06 ± 0.24	99.69 ± 19.68
MDEA III-PCN	7.81 ± 0.48	2.57 ± 0.46	52.04 ± 4.52	5.48 ± 0.86	152.58 ± 35.94
MDEA IV-PCN	7.53 ± 0.56	2.16 ± 0.17	48.08 ± 3.05	4.97 ± 1.36	112.67 ± 24.02

decreased to 20 nm, and the well-stacked nanoclays were broken down into small pieces. MDEA IV–PCN [Fig. 10(c)] also showed a delaminated clay sheet similar to MDEA III–PCN and the clay sheet was partly separated by an intercalated structure. Consequently, MDEA III–PCN and MDEA IV–PCN had better clay dispersion than MMT–PCN in the PET matrix.

From the above results, the study of clay dispersion in PCNs should be investigated by multiple scales, such as micron and submicron levels, because it is possible that clay agglomerates and isolated clay platelets coexist at different scales.

Capillary rheometer

The rheology of various polymer/clay nanocomposites was studied by Giannelis et al.[24] The apparent viscosity increased significantly when nanoclay was incorporated because of its large exposed surface area with increased polymer–clay interaction, even at low nanoclay contents.[25] The apparent melt viscosities of pure PET, MDEA III–PCN, and MDEA IV–PCN are presented in Figure 11. The melt viscosity of these PCNs loaded with only 0.5 wt % clay increased to 88 from 63 Pa s for the pure PET at 1000 s^{-1}. The melt viscosity of both PCNs showed similar behavior in the range of whole shear rates (50–5000 s^{-1}) and the melt viscosity increased by 40% in the shear rate range (100–1000 s^{-1}) when compared to pure PET.

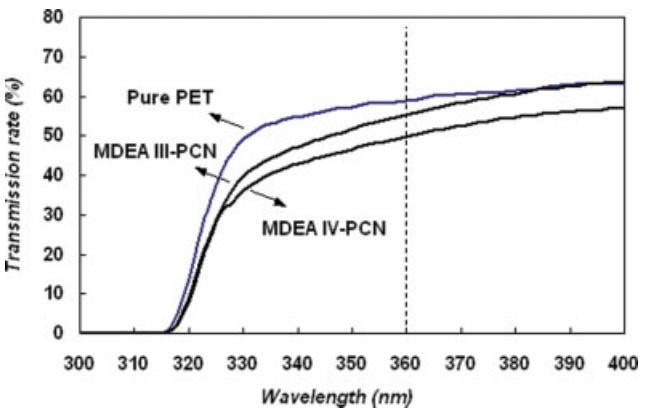

Figure 13 UV transmission spectra of pure PET, MDEA III–PCN, and MDEA IV–PCN. [Color figure can be viewed in the online issue, which is available at www.interscience.wiley.com.]

Tensile properties

Tensile deformation of PET has been studied via neck propagation and strain hardening phenomena.[26–28] In general, polymer nanocomposites exhibit enhanced mechanical strength compared to neat polymers because the dispersed clay layers provide reinforcement in a polymer matrix.[29,30]

The stress–strain curves of pure PET, MDEA I–PCN, MDEA III–PCN, and MDEA IV–PCN are shown in Figure 12; the results of the tensile properties are summarized in Table IV. The tensile strength of MDEA III–PCN was around 52 MPa, but that of pure PET was only 27.5 MPa. The other PCNs (MDEA I–PCN and MDEA IV–PCN) had values similar to that of MDEA III–PCN. The tensile strength of the PCNs was increased by 75–89% compared to pure PET. The fracture behaviors of the PCNs in Figure 12 are quite different from pure PET. The PCNs were fractured with strain hardening phenomena at the end region of the stress–strain curve, but pure PET lacked the strain hardening effect. In other words, the stability of neck propagation in the PCN specimens during cold drawing was increased.

Improvement of the tensile properties in the MDEA III–PCN, such as tensile strength and strain hardening, was caused by the well-dispersed clay structure because the interfacial area between the MDEA III organoclay and PET matrix was higher than other PCNs. Stability enhancement of neck propagation during stress–strain measurements of the PCNs was also presumed to be attributable to the formation of smaller crystallites with the confinement of the partially delaminated clay layers.

Barrier properties

The UV barrier property is a very important factor for food and beverage packaging because UV radiation

TABLE V
UV Barrier Properties of Pure PET, MDEA III-PCNs and MDEA IV-PCN

Sample	IV (dL/g)	Clay content (wt %)	Transmission rate[a] (%)	UV barrier[b] (%)
Pure PET	0.6	0	59	41
MDEA III-PCN	0.6	0.5	55	45
MDEA IV-PCN	0.6	0.5	50	50

[a] The UV transmission rate was measured at 360 nm.
[b] UV barrier = 100(%) − Transmission rate (%).

TABLE VI
OTR Results of Pure PET Sheet and PCN Sheets

Sample	IV (dL/g)	Clay content (wt %)	OTR
Pure PET	0.8	0	6.48
MMT-PCN	0.8	1	3.41
MDEA III-PCN	0.8	1	3.14

OTR, oxygen transmission rate (mm cc/m^2 day).

can induce photooxidation, which has significant effects on the quality of some foods.[31] UV transmission spectra for MDEA III–PCN and MDEA IV–PCN are shown in Figure 13 and the values are summarized in Table V. Taking into account the UV transmission rate of the PCNs at 360 nm, the reduction was 4–9% in relation to pure PET.

The gas barrier property was expressed by the measurement of oxygen permeability through the PCN sheet. A comparison of the OTR values between pure PET and PCN samples is listed in Table VI and shown in Figure 14. The OTR value of the pure PET sheet was 6.48, but the PCN samples had lower OTR values than pure PET. This means that the oxygen barrier property of PCN was improved. The OTR value of MMT–PCN was 3.41 and that of MDEA III–PCN was 3.14. Both of them had 1 wt % clay loading in PET matrix. From the results of the OTR values, the MDEA III–PCN showed an improved oxygen barrier property compared to pure PET.

CONCLUSION

Four different kinds of modified organoclays were prepared for PET. PCNs were synthesized by *in situ* polymerization. They showed intercalated and delaminated clay dispersion. MDEA III organoclay especially had the best clay dispersion among the PCNs. MDEA III–PCN and MDEA IV–PCN both contained bundles of nanoclay with sizes below 20 nm. Compared to pure PET, the melt viscosity and tensile property of PCNs loaded with only 0.5 wt % clay showed significant improvement. In the barrier studies, MDEA III–PCN and MDEA IV–PCN showed enhanced properties for UV and gas barrier. In the case of the UV barrier, the transmission rates of the PCNs at 360 nm decreased by 4–9%. The gas barrier property of MDEA III–PCN loaded with 1 wt % organoclay also showed twofold enhancement when compared to pure PET.

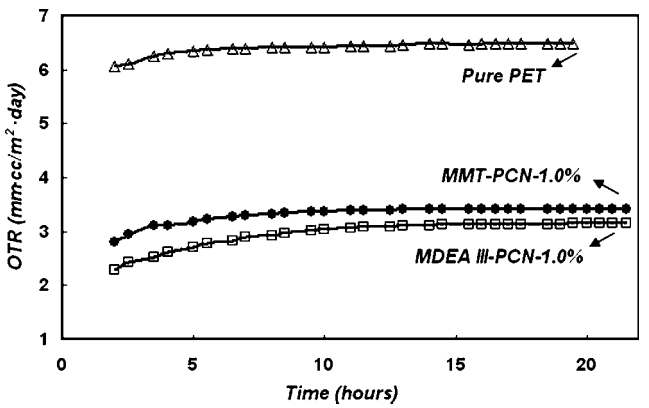

Figure 14 An OTR chart of a pure PET sheet and PCN sheets.

This work was supported by the Industrial Technology Development Fund of the Korea Institute of Industrial Technology Evaluation & Planning.

References

1. Ke, Y.; Long, C.; Qi, Z. J Appl Polym Sci 1999, 71, 1139.
2. Davis, C. H.; Mathias, L. J.; Gilman, J. W.; Schiraldi, D. A.; Shields, J. R.; Trulove, P.; Sutto, T. E.; Delong, H. C. J Polym Sci Part B: Polym Phys 2002, 40, 2661.
3. Saujanya, C.; Imai, Y.; Tateyama, H. Polym Bull 2002, 49, 69.
4. Saujanya, C.; Imai, Y.; Tateyama, H. Polym Bull 2003, 51, 85.
5. Inceoglu, A. B.; Yilmazer, U. Polym Eng Sci 2003, 43, 661.
6. Imai, Y.; Inukai, Y.; Tateyama, H. Polym J 2003, 35, 230.
7. Chang, J. H.; Kim, S. J.; Joo, Y. L.; Im, S. Polymer 2004, 45, 919.
8. Tsai, T.-Y. In Polymer–Clay Nanocomposites; Pinnavaia, T. J.; Beall, G. W., Eds. Wiley: 2000; Chap. 9.
9. Sanchez-Solis, A.; Garcia-Rejon, A.; Manero, O. Macromol Symp 2003, 192, 281.
10. Kim, S. H.; Park, S. H.; Kim, S. C. Polym Bull 2005, 53, 285.
11. Frisk, P.; Laurent, J. U.S. Pat. 5876812, 1999.
12. Frisk, P.; Laurent, J. U.S. Pat. 5972448, 1999.
13. Barbee, R. B.; Matayabas, Jr., J. C.; Gilmer, J. W. U.S. Pat. 6071988, 2000.
14. Choi, W. J.; Kim, S. H.; Kim, Y. J.; Kim, S. C. Polymer 2004, 45, 6045.
15. Ma, Y.; Agarwal, U. S.; Sikkema, D. J.; Lemstra, P. J. Polymer 2003, 44, 4085.
16. Huang, B.; Ito, M.; Kanamoto, T. Polymer 1994, 35, 1329.
17. Huang, B.; Cuculo, J. A.; Tucker, P. A. Polymer 1997, 38, 1101.
18. Huang, B.; Walsh, J. J. Polymer 1998, 39, 6991.
19. Tanem, B. S.; Kamfjord, T.; Augestad, M.; Lovgren, T. B.; Lundquist, M. Polymer 2003, 44, 4283.
20. Sur, G. S.; Sun, H. L.; Lyu, S. G.; Mark, J. E. Polymer 2001, 42, 9783.
21. Bandyopadhyay, S.; Giannelis, E. P. Polym Mater Sci Eng 2000, 82, 208.
22. Chang, J. H.; Seo, B. S.; Hwang, D. H. Polymer 2002, 43, 2969.
23. Bharadwaj, R. K.; Mehrabi, A. R.; Hamilton, C.; Trujillo, C.; Murga, M.; Fan, R.; Chavira, A.; Thompson, A. K. Polymer 2002, 43, 3699.
24. Giannelis, E. P.; Krishnamoorti, R.; Manias, E. Adv Polym Sci 1999, 138, 107.
25. Artzi, N.; Nir, Y.; Narkis, M.; Siegmann, A. J Polym Sci Part B: Polym Phys 2002, 40, 1741.
26. Tanrattanakul, V.; Perkins, W. G.; Massey, F. L.; Moet, A.; Hiltner, A.; Baer, E. Polymer 1997, 38, 2191.
27. Pawlak, A.; Perkins, W. G.; Massey, F. L.; Hiltner, A.; Baer, E. J Appl Polym Sci 1999, 73, 203.
28. Prattipati, V.; Hu, Y. S.; Bandi, S.; Schraldi, D. A.; Hiltner, A.; Baer, E.; Mehta, S. J Appl Polym Sci 2005, 97, 1361.
29. Hasegawa, N.; Okamoto, H.; Kato, M.; Usuki, A.; Sato, N. Polymer 2003, 44, 2933.
30. Kojima, Y.; Usuki, A.; Kawasumi, M.; Fukushima, Y.; Okada, A.; Kurauchi, T.; Kamigaito, O. J Mater Res 1993, 8, 1185.
31. Coltro, L.; Padula, M.; Saron, E. S.; Borghetti, J.; Buratin, A. E. P. Packaging Technol Sci 2003, 16, 15.